Chinese Journal of Chemical Engineering 60 (2023) 205–211

Contents lists available at ScienceDirect

Chinese Journal of Chemical Engineering

journal homepage: www.elsevier.com/locate/CJChE

Full Length Article

Synthesis of an IMF zeolite membrane for the separation of xylene isomer

Wenwen Zhang [1,#], Zhigang Xue [1,#], Liyun Cui [2], Haoliang Gao [2], Di Zhao [2], Rongfei Zhou [1,*], Weihong Xing [1,*]

[1] State Key Laboratory of Materials-Oriented Chemical Engineering, College of Chemical Engineering, Nanjing Tech University, Nanjing 210009, China
[2] Chambroad Chemical Industry Research Institute Co. Ltd., Binzhou 256500, China

ARTICLE INFO

Article history:
Received 6 December 2022
Received in revised form 18 January 2023
Accepted 29 January 2023
Available online 13 March 2023

Keywords:
Membranes
Zeolites
Separation
Xylene
Secondary growth

ABSTRACT

The synthesis of a continuous IMF zeolite membrane was fabricated on tubular substrates by seeded growth for the first time. The straight channels of IMF zeolite with diameters of 0.53–0.59 nm are distinguishable for *p*-xylene from *o*-xylene molecules. Pure IMF-phase high-silica IM-5 zeolite seeds with uniform and fine crystal size were fabricated by a new sonication-assisted aging process. The seeds were coated on the support by dipcoating and induced the formation of continuous membrane. Separation performance in *p*-/*o*-xylene mixture was investigated at various temperature and pressure. The typical IM-5 zeolite membrane had *p*-/*o*-xylene separation factor of 3.7. Our results suggest that IM-5 zeolite is a potentially good membrane material for the separation of xylene mixtures.

1. Introduction

The eight-carbon aromatic fraction obtained from naphtha reforming and steam cracking contains a xylene isomer mixture. The surplus of *o*-xylene (OX) and *m*-xylene (MX) can be converted to the value-added *p*-xylene (PX) by catalytic isomerization [1,2]. The boiling point difference between the components is very small, which makes the separation energy-intensive by the conventional distillation method. Membrane separation is an energy-saving separation technology for gas separation and has been applied industrially for CO_2 separation from natural gas and biogas [3–5]. However, distinguishing PX from OX is more challenging than separating CO_2 from CH_4 by membrane because the physical and chemical properties of the former components are closer.

Zeolite membranes became the promising and ideal membrane materials for gas separation due to their uniform and crystalline micropores [6]. Separation of PX/OX mixtures using zeolite membranes like Zeolite Scony Mobil - five (ZSM-5) is the research hotpot [7–9]. ZSM-5 zeolite (Mobil Five, MFI topology) owns the zigzag pore in *a*-axis direction and the straight one in *b*-axis direction. The *b*-oriented ZSM-5 zeolite membranes are reported for their excellent separation of PX/OX mixture [10–12]. However, the fabrication of zeolite MFI membranes with *b*-axis orientation is very challenging even for the small-area membranes because that the random deposition of nuclei always disturbs the oriented growth [13–16].

Zeolite Institut Français du Pétrole and University of Mulhouse-five (IM-5, IMF topology) has straighter channels (all straight channel in all directions) and a lower framework density (17.5 $T{\cdot}nm^{-3}$) than that of ZSM-5 zeolite (sole straight channel in *b*-axis direction and framework density of 18.4 $T{\cdot}nm^{-3}$). IM-5 had pore diameters of 0.55 nm × 0.56 nm and 0.53 nm × 0.54 nm in the *a*-axis direction, 0.48 nm × 5.4 nm and 0.51 nm × 0.53 nm in the *b*-axis direction and 0.53 nm × 0.59 nm in the *c*-axis direction. The pore size of IMF zeolite is similar to that of MFI zeolite. More importantly, all the channels are straight and connected [17]. The diffusivity of gas molecules through these connected and straight channels should be higher than that through some zigzag channels of ZSM-5 zeolite. It could be not necessary to control the preferential orientation of the crystal layer to obtain a straight-channel membrane if IM-5 forms to continuous membrane. Zeolite framework and channels are considered to be expanded by about 10% in the presence of hydrocarbon molecules [18,19]. The actual size of the IMF zeolite channels is expected to larger than the kinetic diameter of PX (0.59 nm) but smaller than that of OX (0.68 nm) when it is explored in the hydrocarbon mixture, similar to that of MFI zeolite. IM-5 is expected to be a potentially promising membrane material for the PX/OX separation. IM-5 was firstly produced by Benazzi *et al.* [20]. Corma *et al.* [21] studied the catalysis performance of

* Corresponding authors.
E-mail addresses: rf-zhou@njtech.edu.cn (R. Zhou), xingwh@njtech.edu.cn (W. Xing).
# These authors contributed equally to this work.

https://doi.org/10.1016/j.cjche.2023.01.020
1004-9541/

IM-5 and ZSM-5 in the hydroisomerization–hydrocracking of *n*-decane and *m*-xylene isomerization; IM-5 showed higher catalytic activity than ZSM-5. In the subsequent work, they found that IM-5 had better hydrothermal stability during fluid catalytic cracking, resulting in higher activity and lower olefin yields [20] than ZSM-5 zeolite. Wang *et al.* [22] found that the phosphorus modified IM-5 showed better toluene conversion and the selectivity of *p*-xylene than ZSM-5 in the reaction of toluene alkylation with methanol.

There were no reports for the synthesis of the continuous IM-5 membranes yet. In this communication, Continuous IM-5 membranes were fabricated by secondary growth on tubular ZrO_2-Al_2O_3 supports for the first time. Separation performance in PX/OX mixture of the prepared membranes were evaluated.

2. Experimental

2.1. Synthesis of IM-5 seeds

IM-5 was fabricated in a gel with a molar ratio of 17 Na_2O: 60 SiO_2: 1.5 Al_2O_3: 6 NaBr: 10 1,5-bis(methylpyrrolidinyl)pentane: 2400 H_2O according to the Ref. [20] after synthesis modification. The modification was the sonication treatment for the gel in order to prepare uniform and small seed crystals without any impurity phase. For a typical synthesis, 115 mmol NaOH pellets (96.0% by mass, Sinopharm, China), 10 mmol $NaAlO_2$ powder (99% by mass, Wako, Japan) and 204 mmol silica powder (99.99% by mass, Aladdin, China) was dissolved in 146.7 ml deionized water in sequence. And then 34 mmol organic structure-directing agent (OSDA) of 1,5-bis(methylpyrrolidinyl)pentane (50.18% aqueous solution by mass, Guangzhou Dayou Co. Ltd., China) and 20 mmol NaBr (99.0% by mass, Yonghua Chemical Co., Ltd., China) were mixed to obtain the final gel. The effective modification was that the gel was aged by ultrasonic treatment at 353 K for 6 h. The gel was hydrothermally crystallized at 448 K for 7 d to obtain pure-phase nano-sized IM-5 crystals. The organic structure directing agent (OSDA) removal was proceeded by calcining at 853 K for 4 h. The samples without ultrasonic aging were prepared for comparison.

2.2. Seeding procedure

IM-5 seeds were deposited on the outside tubular asymmetric supports by dip-coating approach. The asymmetric supports were supplied by Nanjing Membrane Park Co. and had an α-Al_2O_3 body (porosity: ~30%, OD: 12 mm, ID: 9 mm and average pore size: 1.0 μm) and an active ZrO_2 layer (coating thickness: 20 μm and average pore size: 200 nm). The IM-5 seed suspension was obtained by scattering 0.15 g seeds in 500 g ethanol followed by sonicated for 2 h. Each end of the tube was sealed using silicone plug to prevent the depositing of seeds on the inside surface. The supports were seeding after the programed dip-coating procedure [19] and dried at 333 K overnight.

2.3. Membrane synthesis

The gel mixture for membrane growth has a molar composition of 17 Na_2O: 60 SiO_2: 1.2 Al_2O_3: 6 NaBr: 10 1,5-bis(methylpyrrolidinyl)pentane: 2400 H_2O. The production of the membrane gel was the same with that of the seed gel. The gel for membrane growth was aged with stirring at 353 K for 3 d. Secondary growth of the membrane was proceeded at 448 K for 7 d. The hydrothermal synthesis was repeated to reduce the boundary defects. The OSDA was removed from the IM-5 membrane by calcining at 803 K for 4 h at increasing & declining rates of 0.5 K·min^{-1}.

2.4. Characterization and gas separation

X-ray diffraction (XRD) patterns of seed and membrane samples were measured on a Ultima IV X-ray diffractometer using radiation source of Cu K_α. Scanning electron micrographs (SEM) of the seed and membrane samples were collected using Hitachi S4800 microscope at 5 kV. Thermogravimetric (TG) analyses were performed in air on a NETZSCH STA 409PC thermal analyzer, where weight loss related to the combustion of OSDA was determined from differential scanning calorimetry (DSC). The adsorption experiment for N was performed on a Micromeritics ASAP 2020 analyzer. The structure of IM-5 was characterized by a Fourier transform infrared spectrometry (FT-IR, Thermo Nicolet 8700).

Separation data of IM-5 membranes were recorded by Wicke-Kallenbach (W-K) method with N_2 as sweep gas, the separation system was illustrated schematically in Fig. 1. Two bubblers were used for PX and OX streams, respectively. The carrier gas (N_2) was independently fed to each bubbler and mixed to formed the PX/OX vapor stream. The vapor stream was then fed into membrane module. All the pipelines of the system were kept at 383 K using the heating tape. The total feed flow rate of carrier gas was maintained at 100 ml·min^{-1}, and that of another N_2 sweep gas was 100 ml·min^{-1} at the permeate side. The total pressure on both sides was atmospheric pressure. Note that the composition and pressure of PX and OX in the feed could be regulated by the temperature of bubbler and the flow rate of carrier gas. Usually, the feed partial pressures of PX and OX kept to be ~0.5 kPa. The concentration of the components were analyzed by Shimadzu GC-2014 gas chromatogram with a flame ionization detector. Chromatographic analysis was performed with the internal standard

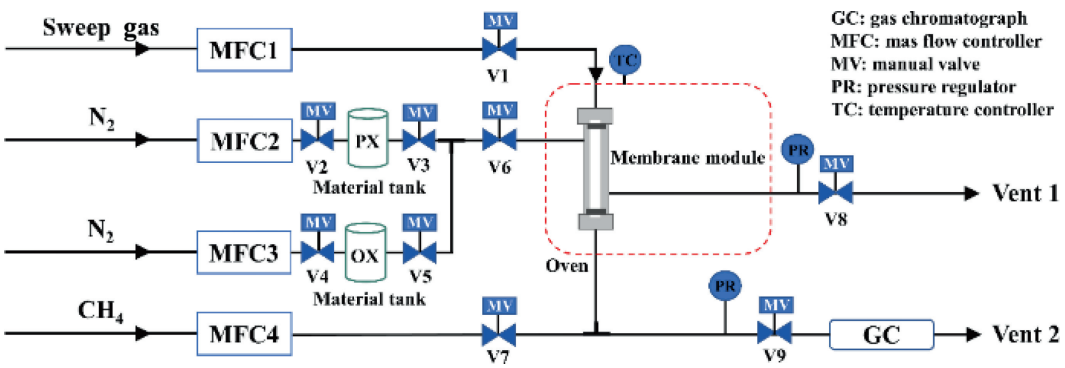

Fig. 1. Schematic diagram of the gas-separation setup for the test of PX/OX mixture.

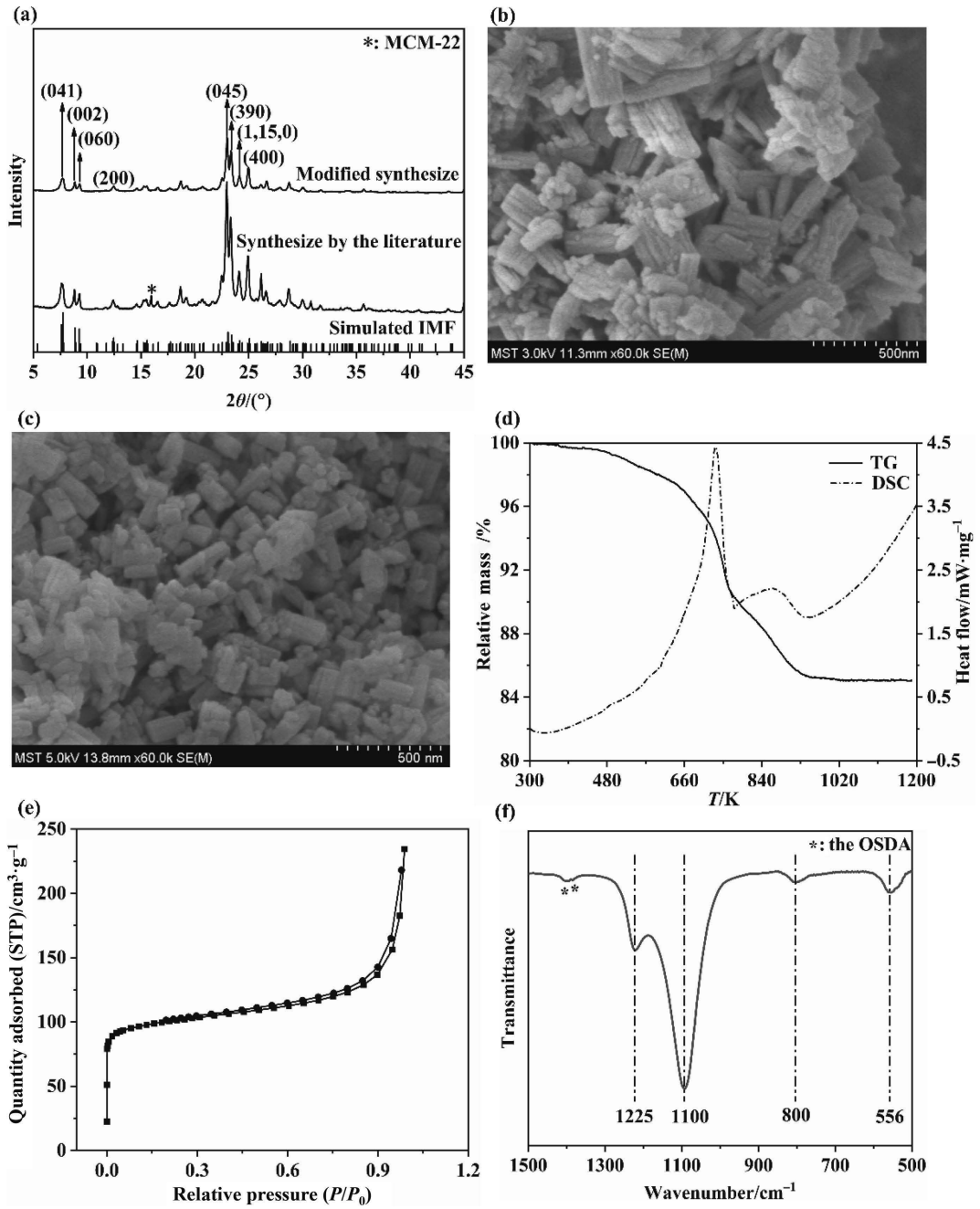

Fig. 2. (a) Powder XRD patterns of simulated IMF, IM-5 fabricated by normal synthesis and modified synthesis, and SEM images of IM-5 fabricated by (b) normal synthesis and (c) modified synthesis, (d) the TG and DSC curves for IM-5 produced by modified synthesis, (e) the N_2 adsorption–desorption isotherms of IM-5 produced by modified synthesis and (f) IR spectra of IM-5 produced by modified synthesis.

method in which the CH_4 was used as the internal standard substance.

The permeance of mixed components is obtained by the following equation:

$$P_i = \frac{N_i}{\Delta P_i} \tag{1}$$

where N_i and ΔP_i are the flux and the pressure drop of composition i, respectively.

The separation factor is calculated as the ratio of the ratios of the PX and OX concentration in the permeate and feed sides as the equation:

$$\mathrm{SF} = \frac{(y_i/y_j)_\mathrm{p}}{(x_i/x_j)_\mathrm{f}} \tag{2}$$

where y_i, y_j, x_i and x_j are the molar ratios of component i (PX) and j (OX) in the permeate (p) and the feed (f) sides, respectively.

3. Results and Discussion

Fig. 2 displays XRD patterns, SEM images, TG curves, adsorption isomer and IR spectra of the prepared IM-5 powders. Two kinds of IM-5 were obtained following the Ref. [20] and after modification with ultrasonic aging, respectively. Pure-phase IM-5 was not

prepared in our case following the literature [20] as shown in Fig. 2 (a). The product was composed of IM-5 as the main phase and mobil composition of matter-twenty-two (MCM-22) as the secondary one identified by XRD. After the synthesis modification using ultrasonic aging, pure IM-5 was obtained. The success on the inhibition of impurity phase of MCM-22 zeolite in the product could be attributed to the aging-improved sonication process. The sonication in the aging process might improve the dissolution of the amorphous alumina and silica precursors. The concentration of the precursors in the solution after enhanced dissolution might be suitable to the nucleation and crystallization of IM-5. And therefore, the formation of the impurity zeolite phase could be inhibited. IM-5 prepared by the two routes had similar column-like morphologies as shown in Fig. 2(b) and (c). The size of the crystals prepared by modified synthesis was more uniform and smaller (~200 nm in length). TG curve in Fig. 2(d) shows that the decomposition of the OSDA occurred at 858 K. The mass loss for the OSDA removal was about 12.3%. Adsorption isomer of N_2 on IM-5 indicates the properties of micropores as shown in Fig. 2(e). It had the BET surface area and the volumes of total pores and micropores of 350 $m^2 \cdot g^{-1}$, 0.36 $cm^3 \cdot g^{-1}$ and 0.15 $cm^3 \cdot g^{-1}$, respectively. The Si/Al ratio of IM-5 seeds was approximately 10 detected by EDX. Fig. 2 (f) shows the IR spectra of IM-5 produced by modified synthesis. The IR bands from the OSDA are marked by asterisks. The absorption peaks at wavenumber of 1225 and 556 cm^{-1} were attributed to external linkage vibrations, which were related to five-membered-ring chains. The one at wavenumber of 1100 cm^{-1} was corresponded to an symmetric stretching of O═Si═O bond, and the one at 800 cm^{-1} to that of Si—O band.

Fig. 3 exhibits SEM images of the zirconia/alumina composite support and the IM-5 membranes after once and twice hydrothermal synthesizes. The active ZrO_2 layer (top layer) had the thickness of approximately 20 μm and average pore size of 200 nm. After once hydrothermal synthesis, the support surface was fully coated by the column-like IM-5 layer with thickness about 800 nm as shown in Fig. 3(c) and (d). The intergrowth behavior was relatively poor and the thickness of the membrane was not uniform. After twice hydrothermal synthesizes, the intergrowth of the zeolite

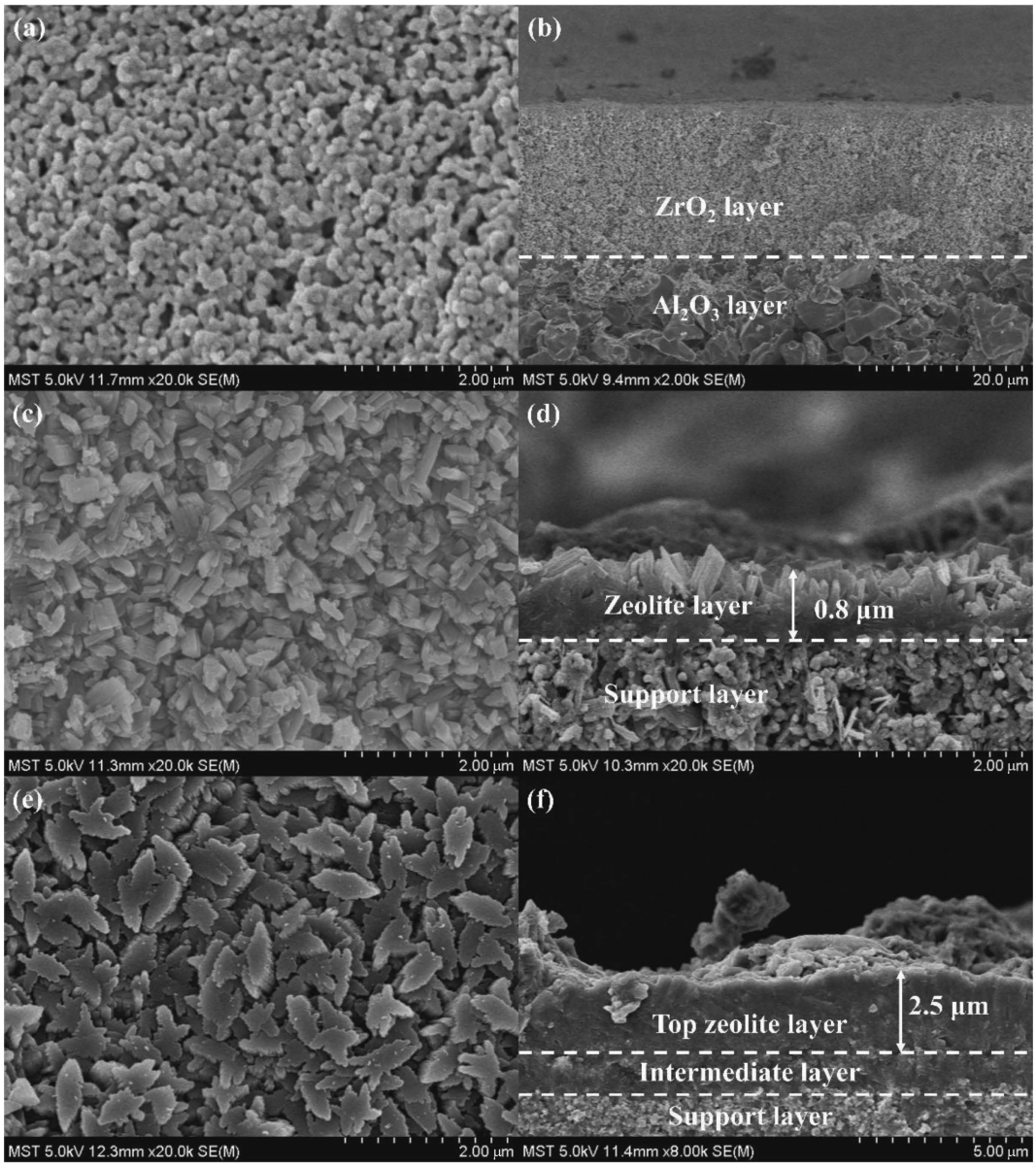

Fig. 3. Electron microscopes of (a, b) the zirconia/alumina composite support and the IM-5 membranes after (c, d) once and (e, f) twice hydrothermal synthesizes.

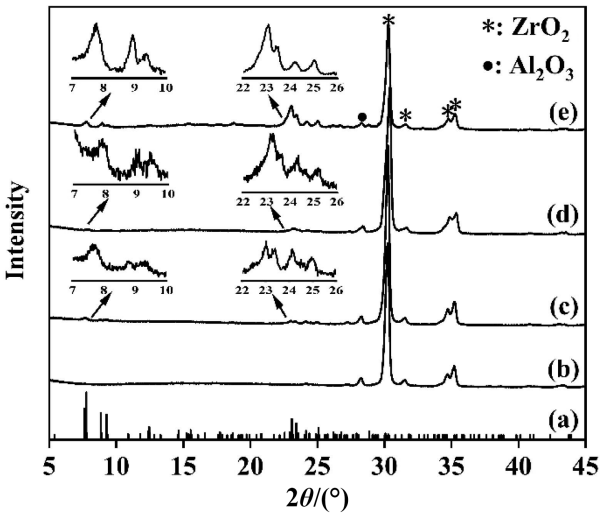

Fig. 4. Powder XRD patterns of (a) simulated IMF peaks, (b) zirconia/alumina composite support, (c) seeded support and the IM-5 membranes after (d) once and (e) twice hydrothermal synthesizes.

layer was greatly improved on the support as shown in Fig. 3(e) and (f). There were a top 2.5-μm-thick IM-5 layer and a dense 0.8-μm-thick intermediate layer on the porous support.

Fig. 4 illuminates the XRD patterns of zirconia/alumina composite support, seeded support and the IM-5 membranes after once and twice hydrothermal synthesizes. The seeded supports had the weak peaks of IM-5 and the strong ones of the supports. IM-5 membranes had more and more obvious peaks of IMF phase with the increase of membrane layers after once and twice hydrothermal synthesizes, indicating that the thickness of zeolite layer increased with synthesis times. No other zeolite phases were found in the XRD patterns of the membranes, suggesting that the obtained membranes are pure IMF (IM-5 herein) phase.

Table 1 presents the separation data of four typical membranes M1−M4 after twice hydrothermal synthesizes for the binary PX/OX (50/50 in mol) mixture. The separation factor and PX permeance of the four membranes varied from 2.3 to 3.7 and from 3.2 to 9.4 × 10^{-8} mol·m^{-2}·s^{-1}·Pa^{-1} at 523 K and 0.5 kPa patrial PX pressure, respectively. It indicated that the membrane had the separation potentials for PX/OX separations. Daramola *et al.* [23] fabricated hollow-fiber ZSM-5 membranes with a maximum PX permeance of 9 × 10^{-9} mol·m^{-2}·s^{-1}·Pa^{-1} and separation factor of 107 at 573 K. A 12-μm-thick *c*-oriented ZSM-5 zeolite membrane displayed separation factor of 5 in PX/OX mixture [24]. A 3-μm-thick *h0h*-oriented ZSM-5 zeolite membrane was reported to have separation factor of 12 [24]. Jeon *et al.* [12] produced ZSM-5 membranes by gel-free secondary growth method and the typical membrane showed a high PX permeance of 5.6 × 10^{-7} mol·m^{-2}·s^{-1}·Pa^{-1} and separation factor of over 2500. Compared with these separation performances in the literatures by ZSM-5 zeolite membranes [12,23,24], our current IM-5 membranes displayed relatively low PX/OX separation factor. It could be ascribed that the boundary defects were produced in the membrane-synthesis and OSDA-removal processes. On one hand, there were only a few literatures to develop the synthesis of IM-5 zeolite and no references for the synthesis of the membranes. Based on the references, pure IM-5 zeolite was still hardly to prepare since the crystallization was not understood clearly. Synthesis of continuous IM-5 membranes was considered to be more difficult than that of popular MFI zeolite membranes. The current membranes after once hydrothermal synthesis had many pinpores and were non-selective. The quality of the uncalcined membranes after twice hydrothermal synthesizes was evaluated by the permeation test using pure N_2. The four membranes had N_2 permeances of (1.9–5.8) × 10^{-9} mol·m^{-2}·s^{-1}·Pa^{-1}, which were only 1/10000–1/3400 of the bare support's permeance, suggesting that there were only a few defect pores. On the other hand, we consider that the formation of defects could be attributed to the different thermal expansion coefficients between zeolite and support layers [25,26]. Even if the current IM-5 membranes displayed relatively poor PX/OX selectivities, we believe that IM-5 could be a good candidate for PX/OX separation once the boundary defects are reduced/eliminated after synthesis modification and optimization of OSDA removal process in our future work.

Separation of PX/OX mixtures through the real micropores of zeolite membranes is always obeyed the adsorption-diffusion mechanism. In the previous study [9,27], zeolite MFI membranes displayed high PX/OX separation factor even if the adsorption loading of the two compositions on the zeolite was similar. The PX-selective separation could be attributed to the relatively fast diffusivity of PX over OX through the 10-member-ring window of zeolite MFI. We consider that similar separation mechanism was for the separation of PX/OX mixture through our 10-membrane-ring IM-5 zeolite membranes. Besides, the separation through the boundary defects was obeyed the mechanisms of viscous flows and Knudsen diffusion. There are no selectivity for PX/OX separation by the two mechanisms.

Fig. 5 displays the influence of feed *p*-xylene partial pressure on the separation data of IM-5 membrane M2. The permeance of PX declined slightly with improving feed xylene partial pressure. The PX/OX separation factor was almost independent of xylene partial pressure due to the increase trend for OX was similar to that for PX. The relationship of temperature and separation data of membrane M2 is shown in Fig. 6. Both PX permeance and separation factor improved with increasing temperature. The highest PX permeance and PX/OX separation factor were 3.5 × 10^{-8} mol·m^{-2}·s^{-1}·Pa^{-1} and 2.9, respectively, in the test temperature range.

Table 1
The separation data of typical IM-5 membranes M1−M4 under optimized conditions by twice hydrothermal synthesizes for the equimolar PX/OX mixture at 523 K and 0.5 kPa *p*-xylene partial pressure.

Membrane No.	N_2 permeance before calcination[①]/10^{-9} mol·m^{-2}·s^{-1}·Pa^{-1}	Mixed-gas permeance/ 10^{-8} mol·m^{-2}·s^{-1}·Pa^{-1}		PX/OX separation factor
		PX	OX	
M1	2.7	7.9	3.0	2.7
M2	5.8	3.5	1.6	2.2
M3	3.7	9.4	4.0	2.3
M4	1.9	3.2	0.87	3.7
Average of M1−M4		6.0 ± 3.1	2.4 ± 1.4	2.7 ± 0.7

[①] Pure N_2 permeance was tested at 298 K and 0.2 MPa(G) and the pure N_2 permeance of the bare support was 2.0 × 10^{-5} mol·m^{-2}·s^{-1}·Pa^{-1}.

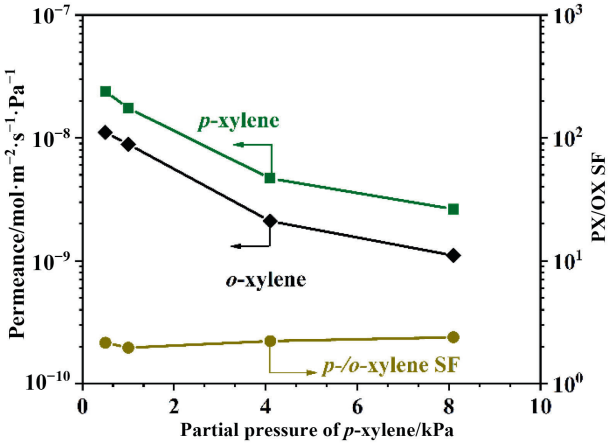

Fig. 5. The relationship of *p*-xylene partial pressure and separation data of typical IM-5 membrane M2 in the PX/OX (50/50 mol) mixture at 548 K.

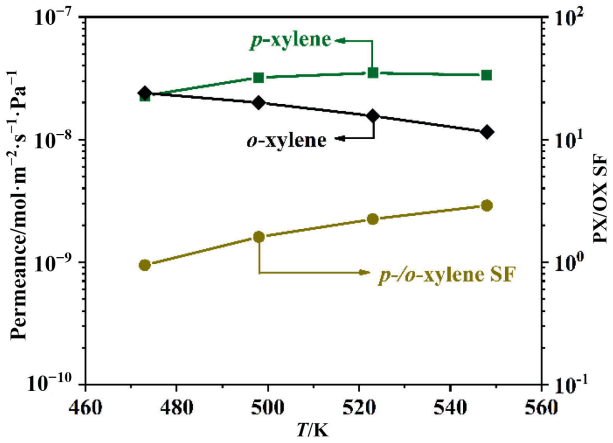

Fig. 6. The relationship of temperature and separation data of typical IM-5 membrane M2 in the PX/OX (50/50 mol) mixture at *p*-xylene partial pressure of 0.5 kPa.

4. Conclusions

In this communication, we have reported the synthesis of a kind of 10-membered-ring IM-5 membrane and the primary separation results for the PX/OX mixture. The membrane synthesis had good reproducibility. Four IM-5 membranes had average PX permeance and PX/OX separation factor of 6.0×10^{-8} mol·m^{-2}·s^{-1}·Pa^{-1} and 2.7 at 523 K, respectively. The results show that IM-5 is a promising membrane material for PX/OX separation. The synthesis modification and post treatment of IM-5 membranes are under way to improve the separation performance of the membranes.

CRediT Authorship Contribution Statement

Wenwen Zhang: Investigation, Methodology. **Zhigang Xue:** Formal analysis, Validation. **Liyun Cui:** Investigation, Writing – review & editing. **Haoliang Gao:** Formal analysis, Validation. **Di Zhao:** Formal analysis, Writing – review & editing, Data curation. **Rongfei Zhou:** Supervision, Funding acquisition, Writing – review & editing. **Weihong Xing:** Writing – review & editing, Conceptualization, Funding acquisition.

Data Availability

No data was used for the research described in the article.

Declaration of Competing Interest

The authors declare that they have no known competing financial interests or personal relationships that could have appeared to influence the work reported in this paper.

Acknowledgements

We acknowledge the supply of the support by Prof. Yiqun Fan and Prof. Minhui Qiu. We acknowledge the financial supports that are from the National Natural Science Foundation of China (21921006, U22A20414 and 21938007), the Natural Science Foundation of Jiangsu Province (BK20220002) and the open project of the State Key Laboratory of China (KL21-04 and D2021FK055).

References

[1] N.M. Tukur, S. Al-Khattaf, Comparison studies of xylene isomerization and disproportionation reactions between SSZ-33, TNU-9, mordenite and ZSM-5 zeolite catalysts, *Chem. Eng. J.* 166 (1) (2011) 348–357.
[2] Y.F. Yeong, A.Z. Abdullah, A. Latif Ahmad, S. Bhatia, Xylene isomerization kinetic over acid-functionalized silicalite-1 catalytic membranes: Experimental and modeling studies, *Chem. Eng. J.* 157 (2–3) (2010) 579–589.
[3] Y. Chen, Y.T. Zhang, C. Zhang, J. Jiang, X.H. Gu, Fabrication of high-flux SAPO-34 membrane on α-Al_2O_3 four-channel hollow fibers for CO_2 capture from CH_4, *J. CO_2 Util.* 18 (2017) 30–40.
[4] R. Krishna, J.M. van Baten, In silico screening of zeolite membranes for CO_2 capture, *J. Membr. Sci.* 360 (1–2) (2010) 323–333.
[5] E. Jang, S. Hong, E. Kim, N. Choi, S.J. Cho, J. Choi, Organic template-free synthesis of high-quality CHA type zeolite membranes for carbon dioxide separation, *J. Membr. Sci.* 549 (2018) 46–59.
[6] J. Caro, M. Noack, Zeolite membranes – Recent developments and progress, *Microporous Mesoporous Mater.* 115 (3) (2008) 215–233.
[7] C.J. Gump, V.A. Tuan, R.D. Noble, J.L. Falconer, Aromatic permeation through crystalline molecular sieve membranes, *Ind. Eng. Chem. Res.* 40 (2) (2001) 565–577.
[8] K. Wegner, J.H. Dong, Y.S. Lin, Polycrystalline MFI zeolite membranes: Xylene pervaporation and its implication on membrane microstructure, *J. Membr. Sci.* 158 (1–2) (1999) 17–27.
[9] H. Sakai, T. Tomita, T. Takahashi, P-Xylene separation with MFI-type zeolite membrane, *Sep. Purif. Technol.* 25 (1–3) (2001) 297–306.
[10] Z.P. Lai, G. Bonilla, I. Diaz, J.G. Nery, K. Sujaoti, M.A. Amat, E. Kokkoli, O. Terasaki, R.W. Thompson, M. Tsapatsis, D.G. Vlachos, Microstructural optimization of a zeolite membrane for organic vapor separation, *Science* 300 (5618) (2003) 456–460.
[11] Z. Lai, M. Tsapatsis, J.P. Nicolich, Siliceous ZSM-5 membranes by secondary growth of *b*-oriented seed layers, *Adv. Funct. Mater.* 14 (7) (2004) 716–729.
[12] M.Y. Jeon, D. Kim, P. Kumar, P.S. Lee, N. Rangnekar, P. Bai, M. Shete, B. Elyassi, H.S. Lee, K. Narasimharao, S.N. Basahel, S. Al-Thabaiti, W.Q. Xu, H.J. Cho, E.O. Fetisov, R. Thyagarajan, R.F. DeJaco, W. Fan, K.A. Mkhoyan, J.I. Siepmann, M. Tsapatsis, Ultra-selective high-flux membranes from directly synthesized zeolite nanosheets, *Nature* 543 (7647) (2017) 690–694.
[13] S. Aguado, E.E. McLeary, A. Nijmeijer, M. Luiten, J.C. Jansen, F. Kapteijn, *b*-Oriented MFI membranes prepared from porous silica coatings, *Microporous Mesoporous Mater.* 120 (1–2) (2009) 165–169.
[14] X.M. Li, Y.S. Yan, Z.B. Wang, Continuity control of *b*-oriented MFI zeolite films by microwave synthesis, *Ind. Eng. Chem. Res.* 49 (12) (2010) 5933–5938.
[15] Y. Liu, Y.S. Li, W.S. Yang, Fabrication of highly *b*-oriented MFI film with molecular sieving properties by controlled In-plane secondary growth, *J. Am. Chem. Soc.* 132 (6) (2010) 1768–1769.
[16] X.F. Lu, Y.W. Yang, J.J. Zhang, Y.S. Yan, Z.B. Wang, Solvent-free secondary growth of highly *b*-oriented MFI zeolite films from anhydrous synthetic powder, *J. Am. Chem. Soc.* 141 (7) (2019) 2916–2919.
[17] C. Baerlocher, F. Gramm, L. Massüger, L.B. McCusker, Z.B. He, S. Hovmöller, X.D. Zou, Structure of the polycrystalline zeolite catalyst IM-5 solved by enhanced charge flipping, *Science* 315 (5815) (2007) 1113–1116.
[18] H. Xiong, Z.Q. Liu, X. Chen, H.Q. Wang, W.Z. Qian, C.X. Zhang, A.M. Zheng, F. Wei, *In situ* imaging of the sorption-induced subcell topological flexibility of a rigid zeolite framework, *Science* 376 (6592) (2022) 491–496.
[19] B. Wang, T.Y. Wu, M. Yu, S.G. Li, R.F. Zhou, W.H. Xing, Highly ordered nanochannels in a nanosheet-directed thin zeolite nanofilm for precise and fast CO_2 separation, *Small* 16 (41) (2020) 2002836.
[20] A. Corma, J. Martínez-Triguero, S. Valencia, E. Benazzi, S. Lacombe, IM-5: A highly thermal and hydrothermal shape-selective cracking zeolite, *J. Catal.* 206 (1) (2002) 125–133.

[21] A. Corma, A. Chica, J.M. Guil, F.J. Llopis, G. Mabilon, J.A. Perdigón-Melón, S. Valencia, Determination of the pore topology of zeolite IM-5 by means of catalytic test reactions and hydrocarbon adsorption measurements, *J. Catal.* 189 (2) (2000) 382–394.
[22] C. Wang, Y.Q. Wang, H.B. Chen, X. Wang, H.Y. Li, C. Sun, L.Y. Sun, C.Y. Fan, X. Zhang, Effect of phosphorus on the performance of IM-5 for the alkylation of toluene with methanol into *p*-xylene, *Comptes Rendus Chimie* 22 (1) (2019) 13–21.
[23] M.O. Daramola, A.J. Burger, M. Pera-Titus, A. Giroir-Fendler, S. Miachon, L. Lorenzen, J.A. Dalmon, Nanocomposite MFI-ceramic hollow fibre membranes *via* pore-plugging synthesis: Prospects for xylene isomer separation, *J. Membr. Sci.* 337 (1–2) (2009) 106–112.
[24] G. Xomeritakis, Z.P. Lai, M. Tsapatsis, Separation of xylene isomer vapors with oriented MFI membranes made by seeded growth, *Ind. Eng. Chem. Res.* 40 (2) (2001) 544–552.
[25] E.R. Geus, J.C. Jansen, H. Vanbekkum, Calcination of large MFI-type single crystals: Part 1. Evidence for the occurrence of consecutive growth forms and possible diffusion barriers arising thereof, *Zeolites* 14 (2) (1994) 82–88.
[26] E.R. Geus, H. Vanbekkum, Calcination of large MFI-type single crystals, Part 2: Crack formation and thermomechanical properties in view of the preparation of zeolite membranes, *Zeolites* 15 (4) (1995) 333–341.
[27] X.H. Gu, J.H. Dong, T.M. Nenoff, D.E. Ozokwelu, Separation of *p*-xylene from multicomponent vapor mixtures using tubular MFI zeolite mmbranes, *J. Membr. Sci.* 280 (1–2) (2006) 624–633.